

**Stability of the quantized circulation of an attractive Bose-Einstein condensate in a rotating torus**

Rina Kanamoto, Hiroki Saito, and Masahito Ueda

*Department of Physics, Tokyo Institute of Technology, Tokyo 152-8551, Japan  
and CREST, Japan Science and Technology Corporation (JST), Saitama 332-0012, Japan*

(Received 14 May 2003; published 20 October 2003)

We investigate rotational properties of a system of attractive bosons confined in a one-dimensional torus. Two kinds of ground states, uniform-density and bright soliton, are obtained analytically as functions of the strength of interaction and of the rotational frequency of the torus. The quantization of circulation appears in the uniform-density state, but disappears upon formation of the soliton. By comparing the results of exact diagonalization with those predicted by the Bogoliubov theory, we show that the Bogoliubov theory is valid at absolute zero over a wide range of parameters. At finite temperatures we employ the exact diagonalization method to examine how thermal fluctuations smear the plateaus of the quantized circulation. Finally, by rotating the system with an axisymmetry-breaking potential, we clarify the process by which the quantized circulation becomes thermodynamically stabilized.

DOI: 10.1103/PhysRevA.68.043619

PACS number(s): 03.75.Hh, 03.75.Kk, 03.75.Lm

**I. INTRODUCTION**

Gaseous Bose-Einstein condensates (BECs) offer a testing ground for superfluid phenomena over a wide range of parameters because of their great flexibility in accommodating various experimental conditions. In particular, the Feshbach technique makes it possible to control the sign and strength of interactions. Furthermore, optical and magnetic traps provide ideal BEC containers, in which microscopic surface rugosities that give rise to dissipation are either absent or can be manipulated as tunable parameters [1]. These experiments have now become possible in low-dimensional systems [2–6] by tightening the confinement in one or two directions. Low-dimensional systems are simple theoretical models for studying vortices, persistent currents, and solitons [7–16]. For the case of attractive interactions, BECs do not collapse but instead form solitons in one-dimensional mesoscopic systems [5,6,14], where the finite-size effect cuts off long-wavelength quantum fluctuations of the phase. Interestingly, a bright soliton can be formed also in two dimensions if the strength of the interaction is made to oscillate rapidly [16,17]. However, much of the physics of superfluidity in an attractive BEC remains to be investigated.

In this paper we study a system of attractive bosons that are confined in a one-dimensional torus [18] under rotation. When the excitation in the radial direction is negligible, such a system is described by the Lieb-Liniger model with attractive interaction [19], in which a rotating term is added to the Hamiltonian and the periodic boundary condition in a finite system is explicitly taken into account. A Hartree-Fock theory [10] shows that the angular momentum of the system exhibits plateaus of the quantized circulation [20–22] as a function of the rotational frequency of the container. We investigate the stability of quantized circulation by employing the Gross-Pitaevskii mean-field theory (MFT), the Bogoliubov theory, and the exact diagonalization of the many-body Hamiltonian. In Refs. [23,24], it is found that quantum fluctuations become significant near the boundary between the uniform and soliton phases in a nonrotating torus, and that the boundary is singular in the Bogoliubov approximation.

This paper shows, however, that when the system is confined in a rotating torus, quantum fluctuations are significant only in the immediate vicinity of a critical point at which a normalized rotational frequency of the container  $\Omega$  is integral and the dimensionless strength of interaction  $\gamma$  is equal to  $-1/2$ . For other values of  $\Omega$  and  $\gamma$ , no singularities appear in physical quantities at the phase boundary. This is because a soliton can be formed without passing through the singular critical point. This paper also points out that the system in the soliton phase does not possess all of the properties that are usually attributed to a superfluid, especially the quantization of circulation.

This paper is organized as follows. In Sec. II, the ground-state wave functions of the system under rotation are derived analytically within the Gross-Pitaevskii MFT. In Sec. III, the effects of quantum fluctuations on quantized circulation are examined based on the Bogoliubov theory and on the exact diagonalization of the many-body Hamiltonian. The results obtained by these two methods will be shown to agree very well, demonstrating the validity of the Bogoliubov theory. In Sec. IV, the circulation is calculated as a function of  $\Omega$  at zero and finite temperatures based on the MFT and on the exact diagonalization method. In Sec. V, we examine the response of the system, which is initially at rest, to a time-dependent axisymmetry-breaking potential in order to clarify the process by which the quantized circulation becomes thermodynamically stabilized. In Sec. VI, the main results of this paper are summarized. In Appendix A, the definitions and inter-relations of elliptic functions and integrals are summarized to make the present paper self-contained. In Appendix B, some limiting behaviors of soliton solutions are discussed for use in the main text. In Appendix C, some properties of the ground state near the phase boundary are discussed.

**II. ANALYTIC SOLUTION OF THE ONE-DIMENSIONAL GROSS-PITAEVSKII EQUATION WITH A ROTATING DRIVE****A. Hamiltonian for the system**

We consider a system of  $N$  identical bosons with mass  $M$  that are confined in a rotating torus with a radius  $R$  and cross

section  $S$ . The angular frequency of rotation is  $2\Omega$  in units of  $\hbar/(2MR^2)$ . The Hamiltonian for the system in the rotating frame of reference is then given by

$$\hat{\mathcal{K}} = \sum_j (\hat{L}_j - \Omega)^2 + \frac{U}{2} \sum_{i,j} \delta(\theta_i - \theta_j), \quad (1)$$

where  $\hat{L}_j \equiv -i\partial/\partial\theta_j$  is the angular-momentum operator,  $\theta$  is the azimuthal angle, and  $U = 8\pi aR/S$  characterizes the strength of interaction with  $a$  being the  $s$ -wave scattering length. Hereafter, the length, energy, and angular momentum are measured in units of  $R$ ,  $\hbar^2/(2MR^2)$ , and  $\hbar$ , respectively. In Eq. (1), we include for convenience the rigid body's kinetic energy  $N\Omega^2$ , which is a constant and only shifts the zero of energy.

The physical properties of the system described by Hamiltonian (1) change periodically with respect to  $\Omega$  [25,26]. To show this, let us consider the Schrödinger equation

$$\hat{\mathcal{K}}(\Omega)\Phi(\{\theta\}) = \mathcal{F}(\Omega)\Phi(\{\theta\}), \quad (2)$$

where  $\{\theta\}$  stands for  $\theta_1, \theta_2, \dots, \theta_N$ , and the many-body wave function satisfies the single-valuedness boundary condition

$$\Phi(\theta_1, \dots, \theta_i, \dots, \theta_N) = \Phi(\theta_1, \dots, \theta_i + 2\pi, \dots, \theta_N), \quad (3)$$

for any  $\theta_i$ . Substituting a transformation

$$\tilde{\Phi}(\{\theta\}) \equiv \exp\left[-i\Omega \sum_j \theta_j\right] \Phi(\{\theta\}), \quad (4)$$

into Eq. (2), we can eliminate the rotating-drive term from the Schrödinger equation as

$$\hat{\mathcal{K}}_0 \tilde{\Phi}(\{\theta\}) = \mathcal{F}(\Omega) \tilde{\Phi}(\{\theta\}), \quad (5)$$

where  $\hat{\mathcal{K}}_0$  is given by

$$\hat{\mathcal{K}}_0 = \sum_j \hat{L}_j^2 + \frac{U}{2} \sum_{i,j} \delta(\theta_i - \theta_j). \quad (6)$$

However, the boundary condition of the wave function is modified as

$$\begin{aligned} \tilde{\Phi}(\theta_1, \dots, \theta_i, \dots, \theta_N) \\ = e^{2\pi i\Omega} \tilde{\Phi}(\theta_1, \dots, \theta_i + 2\pi, \dots, \theta_N). \end{aligned} \quad (7)$$

Because  $\hat{\mathcal{K}}_0$  in Eq. (5) does not depend on  $\Omega$  and the boundary condition (7) is periodic with respect to  $\Omega$  with the period of one, the eigenvalue  $\mathcal{F}(\Omega)$  should be a periodic function of  $\Omega$  with the same period. Since the thermodynamic quantities are specified completely by the energy spectrum, all thermodynamic quantities calculated below, such as Eq. (59), have the same periodic structure.

In the mean-field approximation, we can therefore define a phase winding number  $J$  as

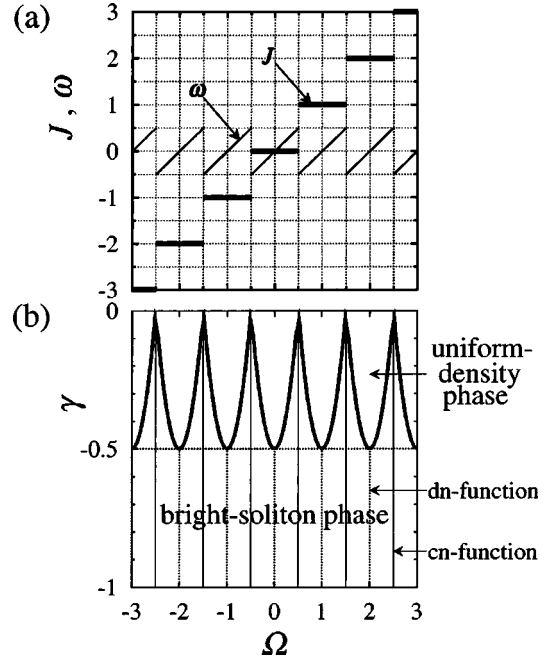


FIG. 1. (a) Phase winding number  $J$  and angular frequency (relative to  $J$ )  $\omega = \Omega - J$  vs  $\Omega$ . (b) Ground-state phase diagram. The bold curve corresponds to the phase boundary determined by Eq. (20):  $\gamma - 2(\Omega - J)^2 + 1/2 = 0$ . The upper and lower regions of the bold curve correspond to the uniform-density phase and the bright-soliton phase, respectively. The winding number  $J$  takes on a constant integer in between the vertical solid lines in (b) and changes by 1 when crossing them. On the solid lines, the ground-state wave function is described by the Jacobian cn function, which has one node. On the vertical dotted lines, the ground-state wave function is described by the Jacobian dn function. In the space between the horizontal dotted line and the bold curve, the uniform-density state is thermodynamically unstable, and below the horizontal dotted line, the uniform-density state is dynamically unstable.

$$J = \left[ \Omega + \frac{1}{2} \right], \quad (8)$$

where the symbol  $[x]$  expresses the maximum integer that does not exceed  $x$ . The angular frequency relative to  $J$  is defined by

$$\omega \equiv \Omega - J, \quad (9)$$

where the range of  $\omega$  is limited to  $-1/2 \leq \omega < 1/2$ . In Fig. 1(a), we plot  $J$  and  $\omega$  against  $\Omega$ .

We first seek the lowest-energy state of the one-dimensional Gross-Pitaevskii equation (GPE) in the rotating frame of reference,

$$[(\hat{L} - \Omega)^2 + 2\pi\gamma] |\psi(\theta)|^2 \psi(\theta) = \mu \psi(\theta), \quad (10)$$

where  $\mu$  is the chemical potential, and a dimensionless parameter

$$\gamma \equiv \frac{UN}{2\pi} \quad (11)$$

gives the ratio of the mean-field interaction energy to the zero-point kinetic energy. The condensate wave function  $\psi(\theta)$  is assumed to obey the periodic boundary condition  $\psi(0) = \psi(2\pi)$ , and is normalized as  $\int_0^{2\pi} |\psi(\theta)|^2 d\theta = 1$ . It is appropriate to assume the form of the solution as

$$\psi(\theta) = \sqrt{\rho(\theta)} e^{i\varphi(\theta)}, \quad (12)$$

where  $\rho$  is the number density and  $\varphi$  the phase.

### B. Uniform-density solution

The stationary state that circulates on a ring with a uniform density is a plane wave,

$$\psi(\theta) = \sqrt{\frac{1}{2\pi}} e^{iJ\theta}, \quad \mu = \omega^2 + \gamma. \quad (13)$$

The stability of the ground state is determined by the sign of the lowest excitation energy. Diagonalizing the Bogoliubov–de Gennes (BdG) equations

$$\begin{aligned} \left[ \left( -i \frac{\partial}{\partial \theta} - \Omega \right)^2 - \mu + 4\pi\gamma |\psi|^2 \right] u_n + 2\pi\gamma \psi^2 v_n &= \lambda_n u_n, \\ \left[ \left( i \frac{\partial}{\partial \theta} - \Omega \right)^2 - \mu + 4\pi\gamma |\psi|^2 \right] v_n + 2\pi\gamma \psi^{*2} u_n &= -\lambda_n v_n, \end{aligned} \quad (14)$$

we obtain the excitation energies  $\lambda_n$  and the corresponding amplitudes  $u_n, v_n$  with positive norms as

$$\lambda_n = \sqrt{n^2(n^2 + 2\gamma)} - 2n\omega, \quad (15)$$

$$u_n = \mathcal{N}_n^+ e^{i(J+n)\theta}, \quad (16)$$

$$v_n = \mathcal{N}_n^- e^{-i(J-n)\theta}, \quad (17)$$

where the normalization constants  $\mathcal{N}_n^\pm$  are determined from the orthonormality condition

$$\int_0^{2\pi} [u_n(\theta) u_m^*(\theta) - v_n(\theta) v_m^*(\theta)] d\theta = \delta_{n,m}, \quad (18)$$

as

$$\mathcal{N}_n^\pm = \sqrt{\frac{1}{4\pi} \left[ \frac{n^2 + \gamma}{\sqrt{n^2(n^2 + 2\gamma)}} \pm 1 \right]}. \quad (19)$$

For repulsive interactions  $\gamma > 0$ , the ground state of Eq. (10) always takes the form of the uniform-density solution (13), since the lowest excitation energy  $\lambda_{-1}$  (for  $-1/2 \leq \omega < 0$ ) or  $\lambda_1$  (for  $0 \leq \omega < 1/2$ ) is positive for all  $\gamma$  and  $\Omega$ . In the attractive case, however, the first excitation energy  $\lambda_1$  or  $\lambda_{-1}$  becomes zero at

$$\gamma - 2\omega^2 + \frac{1}{2} = 0. \quad (20)$$

Figure 1(b) is a phase diagram of the ground states with respect to  $\gamma$  and  $\Omega$ . The bold curve represents the phase boundary (20) of the ground states. The uniform-density solution becomes thermodynamically unstable for  $-1/2 \leq \gamma < 2\omega^2 - 1/2$  (in between the horizontal dotted line and the bold curve) because the first excitation energy becomes negative. On the other hand, the solution becomes dynamically unstable for  $\gamma < -1/2$  (in the lower region of the horizontal dotted line) because the first excitation energy acquires an imaginary part. The uniform-density state is thus stable only when  $\gamma \geq 2\omega^2 - 1/2$  (i.e., in the upper region of the bold curve).

### C. Bright-soliton solution

For  $\gamma < 2\omega^2 - 1/2$  [in the lower region of the bold curve in Fig. 1(b)], a uniform-density state is either thermodynamically or dynamically unstable, but a soliton state is stable. In this section, we derive the ground-state soliton solution of Eq. (10). Several kinds of elliptic integrals and elliptic functions [27] used throughout this paper are defined in Appendix A.

Substituting Eq. (12) into the GPE (10) and taking the real and imaginary parts, we obtain

$$\mu = \Omega^2 - \frac{(\sqrt{\rho})''}{\sqrt{\rho}} + (\varphi')^2 - 2\Omega\varphi' + 2\pi\gamma\rho, \quad (21)$$

$$\varphi'' + 2\varphi' \frac{(\sqrt{\rho})'}{\sqrt{\rho}} - 2\Omega \frac{(\sqrt{\rho})'}{\sqrt{\rho}} = 0. \quad (22)$$

Equation (22) is integrated to give

$$\varphi' = \Omega + \frac{W}{\rho}. \quad (23)$$

Substituting this into Eq. (21) yields

$$\mu\rho^2 = \pi\gamma\rho^3 + V\rho - \left(\frac{\rho'}{2}\right)^2 - W^2. \quad (24)$$

This equation can be rewritten in the form of an elliptic integral

$$\int d\theta = \int \frac{d\rho}{\sqrt{4\pi\gamma\rho^3 - 4\mu\rho^2 + 4V\rho - 4W^2}}, \quad (25)$$

which has formally the same solution as that without the rotating term [15] and is given by

$$\rho(\theta) = \mathcal{N}^2 \left[ \operatorname{dn}^2 \left( \frac{K}{\pi} (\theta - \theta_0) \middle| m \right) - \eta m_1 \right], \quad (26)$$

where  $\operatorname{dn}(u|m)$  is the Jacobian elliptic function,  $0 \leq \eta \leq 1$ , and  $m_1 = 1 - m$ . A constant  $\eta$  is given below in Eq. (29), and the parameter  $m$  is determined later in Eq. (42). We denote the complete elliptic integrals of the first and second kinds as  $K \equiv K(m)$  and  $E \equiv E(m)$ , respectively. Since the soliton breaks the translational symmetry, solution (26) contains a

parameter  $\theta_0$  that specifies the center of mass of the total particles. From the normalization condition, the normalization constant  $\mathcal{N}$  is determined as  $\mathcal{N}^2 = K/[2\pi(E - \eta m_1 K)]$ . Substituting  $\rho$  in Eq. (26) into Eq. (24), we obtain

$$\mathcal{N}^2 = \frac{K}{2\pi(E - \eta m_1 K)} = \frac{K^2}{\pi^3 |\gamma|}, \quad (27)$$

$$\mu = \frac{1}{2\pi^2} (f_d - f_c - f), \quad (28)$$

$$\eta = \frac{f_d}{2m_1 K^2} = 1 - \frac{f_c}{2m_1 K^2}, \quad (29)$$

$$W = -\text{sgn}(\omega) \sqrt{\frac{f f_c f_d}{8\pi^8 \gamma^2}}, \quad (30)$$

where  $f, f_c, f_d$  are defined as

$$f \equiv 2K^2 - 2KE - \pi^2 \gamma, \quad (31)$$

$$f_c \equiv 2m_1 K^2 - 2KE - \pi^2 \gamma, \quad (32)$$

$$f_d \equiv 2KE + \pi^2 \gamma, \quad (33)$$

and  $\text{sgn}$  denotes the sign function such that  $\text{sgn}(\omega) = -1$  when  $-1/2 < \omega < 0$  (i.e.,  $J - 1/2 < \Omega < J$ ) and  $\text{sgn}(\omega) = +1$  when  $0 < \omega < 1/2$  (i.e.,  $J < \Omega < J + 1/2$ ) [see Fig. 1(a)]. The cases of  $\omega = 0$  and  $-1/2$  are treated separately below.

From Eqs. (23) and (26), we find that the phase is given by

$$\varphi(\theta) = \int d\tilde{\theta} \left[ \Omega + \left\{ \frac{K^2}{\pi^3 |\gamma| W} \left[ \text{dn}^2 \left( \frac{K\tilde{\theta}}{\pi} \middle| m \right) - \eta m_1 \right] \right\}^{-1} \right], \quad (34)$$

which can be integrated analytically using relations (A7) and (A10), giving

$$\varphi(\theta) = \Omega \theta - \text{sgn}(\omega) \delta_2^{-1} \Pi \left( n; \frac{K\theta}{\pi} \middle| m \right), \quad (35)$$

where  $\Pi(n; u|m)$  is the elliptic integral of the third kind, and the constants  $n$  and  $\delta_2$  are given by

$$n = \frac{m}{1 - \eta m_1} = \frac{2mK^2}{f}, \quad \delta_2 = K \sqrt{\frac{2f}{f_c f_d}}. \quad (36)$$

Since the wave function is single valued, the phase  $\varphi$  must satisfy

$$\varphi(2\pi) - \varphi(0) = 2\pi J. \quad (37)$$

This condition can be used to determine the value of  $m$  in the following manner. In the present case, the parameters  $m$  and  $n$  satisfy the relation  $m < n < 1$ . Then, using relations (A14)–(A17), the elliptic integral  $\Pi(n; u|m)$  at  $\theta = 2\pi$  reduces to

$$\Pi(n; 2K|m) = 2 \left[ K + \frac{\pi}{2} \delta_2 \{ 1 - \Lambda_0(\varepsilon|m) \} \right], \quad (38)$$

$$\varepsilon = \arcsin \sqrt{\frac{f_c}{m_1 f}}, \quad (39)$$

where  $\Lambda_0$  is Heuman's Lambda function defined in terms of the incomplete elliptic integrals of the first  $F(\varepsilon|m)$  and second  $E(\varepsilon|m)$  kinds as

$$\Lambda_0(\varepsilon|m) = \frac{2}{\pi} [KE(\varepsilon|m_1) - (K - E)F(\varepsilon|m_1)]. \quad (40)$$

The phase at  $\theta = 2\pi$  thus becomes

$$\varphi(2\pi) = 2\pi\Omega - \text{sgn}(\omega) \left[ \sqrt{\frac{2f_d f_c}{f}} + \pi(1 - \Lambda_0) \right]. \quad (41)$$

Using the notation  $\omega \equiv \Omega - J$  instead of  $\Omega$  and  $J$ , condition (37) then leads to

$$2\pi|\omega| = \sqrt{\frac{2f_d f_c}{f}} + \pi(1 - \Lambda_0), \quad (42)$$

which determines the parameter  $m$ . Equation (42) has a solution only when  $\gamma < 2\omega^2 - 1/2$  and  $0 < |\omega| < 1/2$ , i.e., in the region delimited by (but not on) adjacent vertical dotted and solid lines and by the bold curve in Fig. 1(a).

Next let us consider two special cases:  $\omega = 0$  ( $\Omega$  is equal to integer  $J$ , i.e., on the vertical dotted lines) [see Fig. 1(b)], and  $|\omega| = 1/2$  ( $\Omega$  is equal to half integer  $J + 1/2$ , i.e., on the vertical solid lines). The ground-state wave function given by Eqs. (26) and (35) is simplified when  $|\omega| = 0$  and  $|\omega| = 1/2$  according to the limiting values of several parameters discussed in Appendix B.

When  $\omega = 0$ , the amplitude  $\sqrt{\rho(\theta)}$  reduces to the Jacobian elliptic function  $\text{dn}(u|m)$  and the phase  $\varphi(\theta)$  reduces to  $J\theta$ ,

$$\psi(\theta) = \sqrt{\frac{K^2}{\pi^3 |\gamma|}} \text{dn} \left( \frac{K(\theta - \theta_0)}{\pi} \middle| m \right) e^{iJ\theta}. \quad (43)$$

Substituting this solution into the GPE (10) yields the chemical potential

$$\mu = -\frac{K^2}{\pi^2} (1 + m_1) \quad (44)$$

and an equation

$$f_d = 2KE + \pi^2 \gamma = 0, \quad (45)$$

which determines the parameter  $m = 1 - m_1$  only when  $\gamma < -1/2$ . The  $\text{dn}$  solution includes the ground state in the rest container with  $\Omega = 0$ .

When  $|\omega| = 1/2$ , the amplitude is given by the Jacobian elliptic function  $\text{cn}(u|m)$ , and  $\varphi(\theta)$  reduces to  $(J + 1/2)\theta$ ,

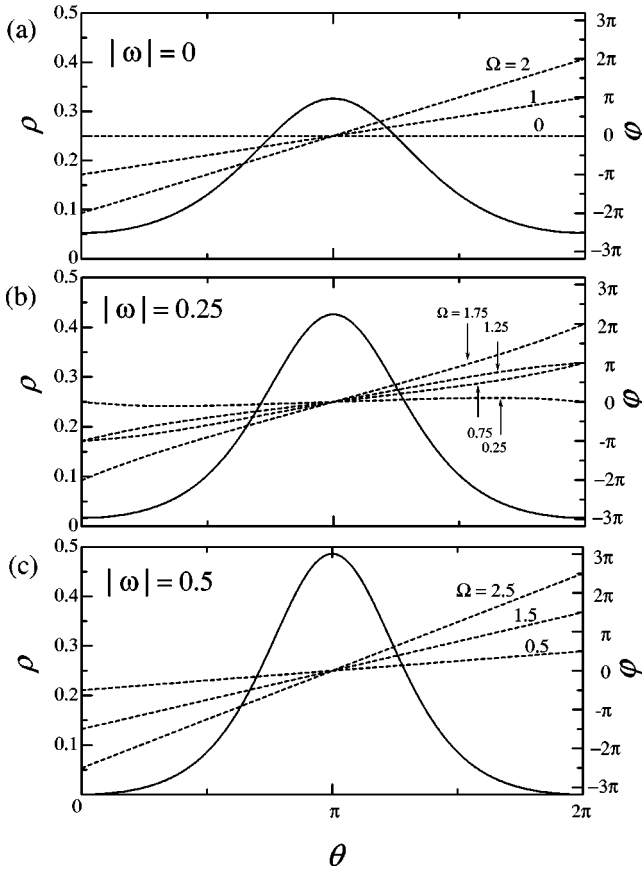


FIG. 2. Densities  $\rho$  (solid curves) and phases  $\varphi$  (dotted curves) for several values of angular frequency  $\omega$  and phase winding number  $J = \Omega - \omega$  with  $\gamma = -0.55$ . The density depends only on  $|\omega|$ . The phase difference  $\varphi(\theta + 2\pi) - \varphi(\theta)$  is given by  $2\pi J$  in panels (a) and (b), and by  $2\pi J + \pi$  in panel (c) because at  $|\omega| = 0.5$  the wave function has a node at which the phase jumps by  $\pi$ .

$$\psi(\theta) = \sqrt{\frac{K^2 m}{\pi^3 |\gamma|}} \text{cn}\left(\frac{K(\theta - \theta_0)}{\pi} \middle| m\right) e^{i(J+1/2)\theta}. \quad (46)$$

The chemical potential and the equation that determines the parameter  $m$  are obtained as

$$\mu = -\frac{K^2}{\pi^2}(1 - 2m_1), \quad (47)$$

$$f_c = 2m_1 K^2 - 2KE - \pi^2 \gamma = 0. \quad (48)$$

Equation (48) has a solution only when  $\gamma < 0$ . The wave function (46) has a node at  $\theta = \theta_0 + \pi$ , and the phase jumps by the amount of  $\pi$  at the node. With increasing  $\Omega$  adiabatically, the vortex enters the ring through this node.

#### D. Ground-state properties

To illustrate the  $\Omega$  dependence of the soliton solution, Fig. 2 shows the densities and the phases for  $\gamma = -0.55$ , where the integral constant for the phase is chosen so that  $\varphi(\pi) = 0$ . The density profiles of the solitons depend only on the relative angular frequency  $|\omega|$ . As the strength of inter-

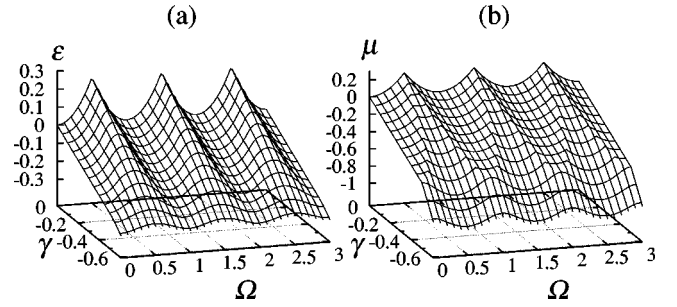


FIG. 3. (a) Ground-state energy  $\mathcal{E}$  per atom and (b) chemical potential  $\mu$ . Both decrease monotonically with increasing  $|\gamma|$  and are periodic with respect to  $\Omega$ .

action is increased, the parameter  $m$  approaches unity (see Fig. 12 in Appendix B) for all  $\omega$ . In the limit of  $m \rightarrow 1$ , both  $\text{dn}(u|m)$  and  $\text{cn}(u|m)$  become  $\text{sech}u$ , which is a soliton solution in infinite space [14].

The ground-state energy  $\mathcal{E}$  per atom of the uniform-density state is given by

$$\mathcal{E} = \omega^2 + \frac{\gamma}{2}, \quad (49)$$

and that of the soliton is given by

$$\begin{aligned} \mathcal{E} = \gamma + \frac{K[3E - (1 + m_1)K]}{\pi^2} \\ + \frac{2K^2[3E^2 - 2(1 + m_1)KE + m_1 K^2]}{3\pi^4 \gamma}. \end{aligned} \quad (50)$$

Equation (50) reduces to the energy of the dn solution in the limit  $\omega \rightarrow 0$  as

$$\mathcal{E} = -\frac{K^2[(1 + m_1)E + m_1 K]}{3\pi^2 E}, \quad (51)$$

and to that of the cn solution in the limit  $|\omega| \rightarrow 1/2$  as

$$\mathcal{E} = -\frac{K^2[(1 - 2m_1)E - m_1(2 - 3m_1)K]}{3\pi^2(E - m_1 K)}. \quad (52)$$

The ground-state energy per atom  $\mathcal{E}$  and the chemical potential  $\mu$  are shown in Figs. 3(a) and 3(b). For a given  $\gamma$ , the ground-state energy  $\mathcal{E}$  reaches minima for integer  $\Omega$  and maxima for half integer  $\Omega$ , and is smooth everywhere. In the regime  $\gamma < -1/2$ , the chemical potential  $\mu$  becomes maximal for integer  $\Omega$  and minimal for half integer  $\Omega$ , and has kinks at the phase boundaries given by  $\gamma - 2(\Omega - J)^2 + 1/2 = 0$ . The phase-transition type is the same as that in the nonrotating case [23]: at the phase boundary (i)  $\mathcal{E}$  is smooth, the first derivative of  $\mathcal{E}$  with respect to  $\gamma$  or  $\Omega$  has a kink and the second derivative of  $\mathcal{E}$  has a jump and (ii)  $\mu$  has a kink and the first derivative of  $\mu$  has a jump. The behaviors of these quantities near the phase boundary are detailed in Appendix C.

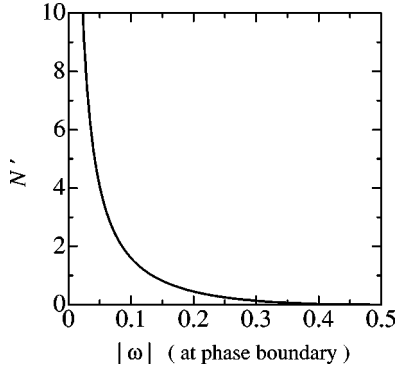


FIG. 4. Quantum depletion  $N'$  [Eq. (55)] at the phase boundary calculated by the Bogoliubov theory.

### III. EFFECTS OF QUANTUM FLUCTUATIONS

Without rotation, the quantum depletion diverges at  $\gamma = -1/2$ , at which point the lowest excitation energy obtained by the Bogoliubov theory becomes gapless. This requires a modification of the MFT [23,24]. We investigate here whether or not in the presence of rotation there is such a singular point at which the effects beyond the Bogoliubov theory are significant.

We evaluate the depletion of the condensate which is calculated according to the Bogoliubov theory as

$$N' = \int_0^{2\pi} \sum_{n \neq 0} |v_n(\theta)|^2 d\theta, \quad (53)$$

where  $v_n(\theta)$  is the hole amplitude in the BdG equation (14). If  $N'/N$  is of the order of unity, the validity of the Bogoliubov theory is not ensured. Since the excitation in the uniform-density regime is contributed mainly by the excitation with quantum number 1, the depletion in the uniform-density regime becomes

$$N' \approx \frac{1 + \gamma}{\sqrt{1 + 2\gamma}} - 1. \quad (54)$$

At the phase boundary  $\gamma = 2\omega^2 - 1/2$ , Eq. (54) reduces to

$$N' \approx \omega + \frac{1}{4\omega} - 1, \quad (55)$$

which is shown in Fig. 4. The quantum depletion diverges at the phase boundary with  $\omega = 0$  and  $\gamma = -1/2$ . However, as  $|\omega|$  is increased,  $N'$  at the phase boundary decreases and the depletion becomes much less pronounced, as shown in Fig. 4. This result is also inferred from Fig. 1(b). The uniform-density state becomes dynamically unstable below the horizontal dotted line  $\gamma = -1/2$ , and this line touches the phase boundary (the bold curve) at  $\omega = 0$ .

We compare low-lying energy levels obtained by the Bogoliubov theory with those obtained by the exact diagonalization of the many-body Hamiltonian (1). Figure 5 shows the Bogoliubov spectra  $\lambda_n$  obtained by the BdG equation (14) as a function of the strength of interaction for angular frequencies  $|\omega| = 0, 0.2$ , and 0.5. The curves represent the

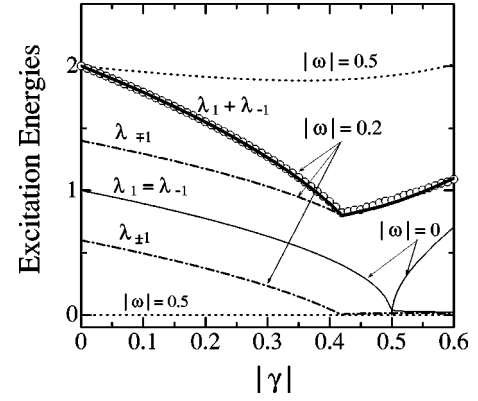


FIG. 5. Bogoliubov spectra  $\lambda_n$  for  $|\omega| = 0$  (solid curve),  $|\omega| = 0.2$  (dashed-and-dotted curves), and  $|\omega| = 0.5$  (dotted curves). The (quasi-) zero-energy levels in the soliton regime correspond to the Goldstone modes associated with the breaking of the translation symmetry due to soliton formation. The open circles show the excitation spectrum  $\mathcal{E}_1(\mathcal{L}_0) - \mathcal{E}_0(\mathcal{L}_0)$  obtained by the exact diagonalization of Hamiltonian (57) for  $N = 500$  with  $|\omega| = 0.2$ . This spectrum agrees with the Bogoliubov spectrum  $\lambda_1 + \lambda_{-1}$  (bold curve) even at the phase boundary  $|\gamma| = 0.42$ .

excitation energies from the uniform-density state for  $|\gamma| < -2\omega^2 + 1/2$ , and those from the soliton state for  $|\gamma| > -2\omega^2 + 1/2$ . All levels are continuous at the boundaries  $|\gamma| = -2\omega^2 + 1/2$ , thus indicating a smooth crossover between the uniform-density state and the soliton state. When  $\omega = 0$  (solid curves),  $\lambda_1$  and  $\lambda_{-1}$  are degenerate in the uniform-density regime, but in the soliton regime ( $|\gamma| > 0.5$ ) they bifurcate into two branches, the first excited state and a Goldstone mode. The Goldstone mode, which is associated with the breaking of translation symmetry, boosts the soliton along the ring without increasing the energy. As  $|\omega|$  is increased from zero (dashed-and-dotted curves), the degeneracy is lifted by rotation.

Next we calculate the low-lying energy levels by the exact diagonalization of the many-body Hamiltonian to see how they deviate from the Bogoliubov spectra near the phase boundary. The diagonalization procedure is the same as that without rotation [23]. We denote the number of atoms with angular momentum  $k$  as  $n_k$  and prepare the plane-wave bases as  $|n_{l_0-l_c}, \dots, n_{l_0-1}, n_{l_0}, n_{l_0+1}, \dots, n_{l_0+l_c}\rangle$ , where  $l_0 = J$  is the angular momentum of the condensate and  $l_c$  is the cutoff. Within the subspace in which the particle number and the total angular momentum are conserved as

$$\sum_{k=l_0-l_c}^{l_0+l_c} n_k = N, \quad \sum_{k=l_0-l_c}^{l_0+l_c} k n_k = \mathcal{L}, \quad (56)$$

we perform the diagonalization of Hamiltonian (1), which is rewritten in second quantized form as

$$\hat{\mathcal{K}} = \sum_l (l - \Omega)^2 \hat{c}_l^\dagger \hat{c}_l + \frac{\gamma}{2N} \sum_{klmn} \hat{c}_k^\dagger \hat{c}_l^\dagger \hat{c}_m \hat{c}_n \delta_{m+n-k-l}. \quad (57)$$

We denote the angular momentum of the ground state as  $\mathcal{L}_0$ , which gives the lowest-energy eigenvalue, and the ground-state energy as  $\mathcal{E}_0(\mathcal{L}_0)$ . The open circles in Fig. 5 show the excitation spectrum  $\mathcal{E}_1(\mathcal{L}_0) - \mathcal{E}_0(\mathcal{L}_0)$  obtained by the diagonalization of Hamiltonian (57) for  $N=500$  and  $|\omega|=0.2$  with cutoff  $l_c=1$ . The results agree very well with the Bogoliubov spectrum  $\lambda_1 + \lambda_{-1}$  (we represent here only the excitations that conserve the total angular momentum  $\mathcal{L}_0$ ). We can also confirm that the difference between the Bogoliubov spectrum and the exact one becomes even smaller as  $|\omega|$  moves further away from zero. This is consistent with the analysis of the depletion of the condensate. The Bogoliubov theory is thus vindicated, except for  $\gamma \approx -1/2$  and  $\Omega \approx J$ .

#### IV. QUANTIZED CIRCULATION AT ZERO AND FINITE TEMPERATURES

##### A. Quantized circulation at zero temperature

A superconductor has no magnetic flux when the applied magnetic field is below a critical value. The analog of this Meissner effect in a neutral superfluid system is the Hess-Fairbank effect [20], in which the system is not set into rotation when the frequency  $\Omega$  of a rotating drive is below a critical value  $\Omega_c$ . When  $\Omega$  exceeds  $\Omega_c$ , the circulation of the system, which is defined as the integral of the superfluid velocity along a closed contour, is quantized in units of  $h/M$  with  $M$  being the atomic mass [21,22]. This is analogous to the case of a type-II superconductor in which quantized vortices enter the system when the external magnetic field exceeds the lower critical field  $H_{c1}$ . The applied magnetic field and the magnetic flux in the superconductor correspond to the rotating drive and the angular momentum  $\langle \hat{L} \rangle$  of the superfluid, respectively.

We calculate the angular momentum of the ground state  $\langle \hat{L} \rangle_0 = N \int_0^{2\pi} \psi^*(\theta) (-i \partial_\theta) \psi(\theta) d\theta$ , where  $\psi$  is the mean-field solution (13) or (26) and (35) obtained in Sec. II. The resulting analytical expression for the expectation value of  $\hat{L}$  per atom is

$$\langle \hat{L} \rangle_0 / N = \begin{cases} J, & \gamma \geq 2\omega^2 - 1/2, \\ J + \omega + 2\pi W, & \gamma < 2\omega^2 - 1/2, \end{cases} \quad (58)$$

where  $W$  is given in Eq. (30) [see also Fig. 11(a)]. In the limits of  $|\omega| \rightarrow 0$  and  $|\omega| \rightarrow 1/2$ ,  $J + \omega + 2\pi W$  reduces to  $J$  and  $J + 1/2$ , respectively. Equation (58) is shown in Fig. 6 as a function of  $\Omega$  and  $\gamma$ , where the plateaus correspond to the uniform-density regime and the crossover regions between plateaus correspond to the soliton regime. For  $\gamma < -1/2$ , the stable uniform-density state does not exist and the plateaus disappear.

Since the quantum fluctuation is small, Eq. (58) correctly describes the ground-state angular momentum except for  $\gamma \approx -1/2$  and  $\Omega \approx J$ . Both the Hartree-Fock theory [10] and the Monte Carlo calculation [28] show that this system exhibits the Hess-Fairbank effect in a certain parameter regime, which is consistent with our results.

We briefly comment on the case of repulsive interaction ( $\gamma > 0$ ). According to the MFT, the ground state with repul-

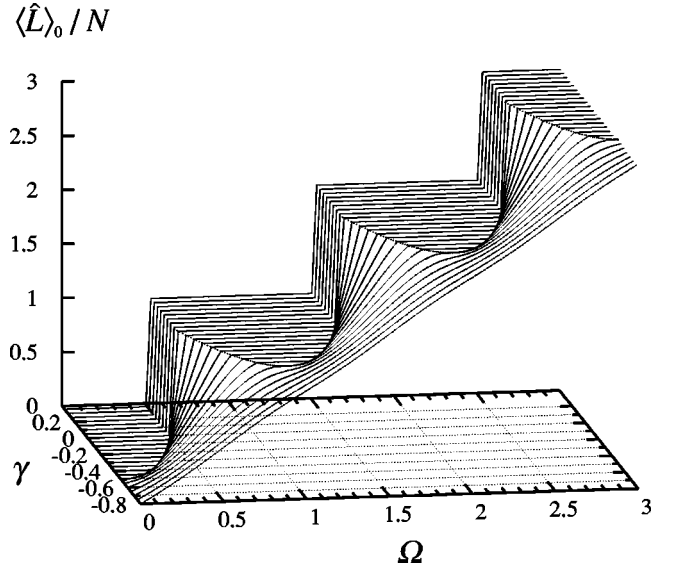


FIG. 6. Expectation value of the angular momentum per atom at zero temperature. The plateau regions correspond to  $\gamma \geq 2(\Omega - J)^2 - 1/2$ . When  $\gamma \leq -0.5$ , the plateaus disappear.

sive interaction has a uniform density for all parameters. The expectation value of the angular momentum then increases stepwise like the noninteracting case, as demonstrated in Fig. 6 with  $\gamma=0$ . The repulsive bosons do not prefer the mixing of different angular-momentum states since it costs the Fock exchange energy.

When  $\Omega$  is controlled in a time-dependent manner, the response to the external rotation displays hysteretic behavior, which is possible only when the energy structure has at least two minima separated by a free-energy barrier [29].

We suppose that  $\Omega$  is increased from zero to one and then decreased back to zero, along the arrows shown in Fig. 7. Unlike the soliton regime for the attractive case, the angular momentum is a good quantum number for the repulsive case. These quantum numbers are shown in parentheses in Fig. 7. When  $\Omega$  is increased from zero, the angular momentum per atom  $\langle \hat{L} \rangle_0 / N$  remains zero until the boundary between II and III is reached, and then jumps to one at the boundary since the two states  $1/\sqrt{2\pi}$  and  $e^{i\theta}/\sqrt{2\pi}$  are divided by a free-

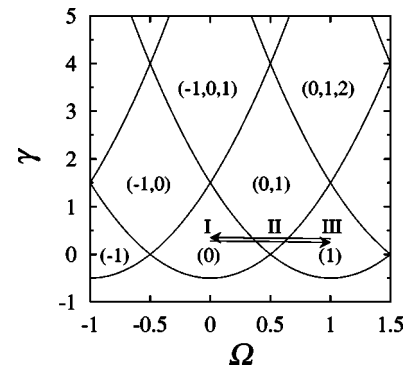


FIG. 7. Angular-momentum quantum numbers for repulsive interactions. The curves are  $\gamma - 2(\Omega - J)^2 + 1/2 = 0$  for  $J = -2, -1, 0, 1, \text{ and } 2$ .

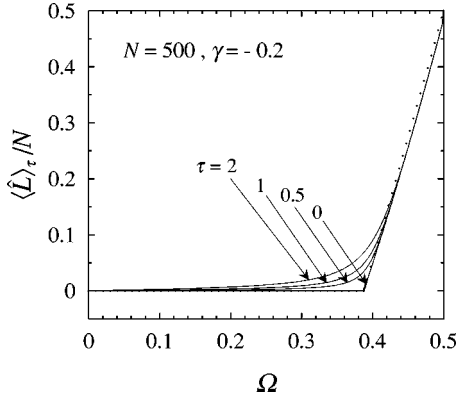


FIG. 8. Angular momentum per atom for  $\gamma = -0.2$  and  $N = 500$  at temperatures  $\tau = 0, 0.5, 1$ , and  $2$  obtained by diagonalization of Hamiltonian (57). The plot shows the result of the mean-field theory at  $\tau = 0$ .

energy barrier in regime II. When  $\Omega$  is decreased from one,  $\langle \hat{L} \rangle_0 / N$  is initially one and remains so until the boundary between I and II is reached, at which point it jumps to zero at the boundary. Thus the hysteresis of  $\langle \hat{L} \rangle$  for the external rotation  $\Omega$  appears. The energy barrier is explicitly obtained by the microscopic calculation of Hamiltonian (57) in Ref. [29].

### B. Quantized circulation at finite temperature

We examine the effect of thermal fluctuations on the quantized circulation at finite temperature. The total angular momentum of the system is obtained from the derivative of free energy  $\mathcal{F}$  with respect to  $\Omega$  as

$$\langle \hat{L} \rangle_\tau = -\frac{1}{2} \frac{\partial \mathcal{F}}{\partial \Omega} + N\Omega, \quad (59)$$

where

$$\tau = \frac{k_B T}{\hbar^2 / (2MR^2)} \quad (60)$$

is a dimensionless temperature with  $k_B$  being the Boltzmann constant,  $\langle \cdots \rangle_\tau$  denotes the ensemble average at temperature  $\tau$ , and the second term in Eq. (59) corresponds to the angular momentum of the rigid body arising from the constant term of Hamiltonian (1).

To evaluate the free energy, we employ the exact diagonalization method of the many-body Hamiltonian. All low-lying levels  $\mathcal{E}_n$  have been obtained in Sec. III, and we use them to calculate the free energy

$$\mathcal{F} = -\tau \ln \sum_n e^{-\mathcal{E}_n / \tau}. \quad (61)$$

Figure 8 shows the angular momentum for several temperatures calculated from Eqs. (59) and (61), where the mean-field result at  $\tau = 0$  is also presented for comparison (dotted lines). At absolute zero, the result obtained by the exact di-

agonalization agrees well with the mean-field result. This supports the validity of the MFT consistent with the results in Sec. III. As the temperature increases, thermal excitations wash out the edge of the circulation step, and the angular momentum of the system approaches that of a classical fluid, i.e.,  $\langle \hat{L} \rangle_\tau = N\Omega$ .

In the present paper, we have focused on the properties near  $\tau = 0$  in this calculation. In principle, however, this method can be extended to higher temperatures by increasing the cutoff angular momentum, as long as the excitations of radial modes are negligible. Near  $|\omega| \approx 1/2$ , however, the results of diagonalization are less accurate than they are at  $\omega \approx 0$ , since more bases are needed in order to allow the state to have a node. In that case, the accuracy can be improved by increasing the cutoff angular momentum.

Finally, we consider an experimental situation. A torus trap may be set up by Laguerre-Gaussian beams [18] or the technique of microelectronic chips [30]. To be concrete, let us consider  ${}^7\text{Li}$ ; then Eq. (60) leads to

$$T \approx 34 \frac{\tau}{(R[\mu\text{m}])^2} [\text{nK}]. \quad (62)$$

Thus for a torus with  $R = 1 \mu\text{m}$ ,  $\tau = 2$  in Fig. 8 corresponds to  $T = 68 \text{ nK}$ , which can be achieved with the current experimental techniques.

### V. PREPARATION OF THE GROUND STATE BY A STIRRING POTENTIAL

Rotation of the system can actually be driven by a potential that breaks the axisymmetry of the system. As a concrete example, we consider a time-dependent potential

$$V(\theta, t) = V_0 \cos(\theta - 2\Omega t), \quad (63)$$

which stirs the system with angular frequency  $2\Omega$ , and we fix the amplitude of the potential as  $V_0 = 10^{-3}$ . We take as an initial state  $\psi(\theta, t=0) = 1/\sqrt{2\pi}$  with a fixed strength of interaction  $\gamma = -1/4$ , and let the system evolve in time according to the GPE,

$$i \frac{\partial}{\partial t} \psi(\theta, t) = \left[ -\frac{\partial^2}{\partial \theta^2} + V(\theta, t) + 2\pi\gamma |\psi(\theta, t)|^2 \right] \psi(\theta, t). \quad (64)$$

Figures 9(a)–9(c) show the time evolution of the angular momentum of the condensate and that of the amplitude  $|\psi(\theta = \pi, t)|$ . One of the phase boundaries for  $\gamma = -1/4$  determined by Eq. (20) is  $\Omega_{\text{cr}} = \sqrt{1/8} \approx 0.354$ . As  $\Omega$  nears  $\Omega_{\text{cr}}$ , the stirring potential causes a significant growth in density as shown in Fig. 9(c). Figure 9(d) plots the maximum amplitude  $|\psi(\theta_0)|$  as a function of  $\Omega$ , which shows the resonance induced near the phase boundary. However, the angular momentum of the system oscillates without damping, and the system does not reach any stationary state.

To achieve a stationary state, we must introduce energy dissipation. We therefore study the time evolution of the system according to a generalized GPE [31,32],

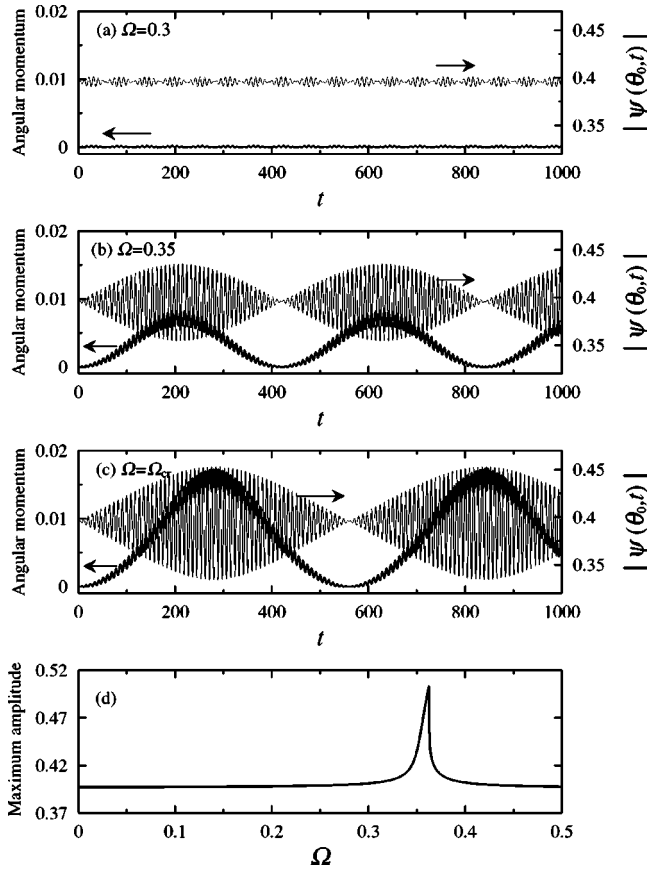


FIG. 9. Time evolution of the angular momentum of the condensate (bold curves) and that of the amplitude  $|\psi(\theta_0, t)|$  at  $\theta_0 = \pi$  (solid curves) driven by a time-dependent stirring potential (63) with  $\gamma = -1/4$  for (a)  $\Omega = 0.3$ , (b)  $\Omega = 0.35$ , and (c)  $\Omega = \Omega_{cr}$ . Note that the oscillations of the density and angular momentum are enhanced close to  $\Omega_{cr} = \sqrt{1/8} \approx 0.354$ . (d) Maximum amplitude of the wave function as a function of  $\Omega$ .

$$(i - \Gamma) \frac{\partial}{\partial t} \psi(\theta, t) = \left[ \left( i \frac{\partial}{\partial \theta} + \Omega \right)^2 + V_0 \cos \theta + 2\pi\gamma |\psi(\theta, t)|^2 \right] \psi(\theta, t), \quad (65)$$

where  $\Gamma$  is a phenomenological damping constant. Figure 10(a) shows the time evolutions of the angular momentum for several values of the angular frequency of stirring with  $\Gamma = 0.1$ . The system acquires a finite angular momentum, and the magnitude of the absorbed angular momentum converges to that of the thermodynamically stable state, as shown in Fig. 10(b). We note that as long as  $\Omega$  lies in the same plateau region, the angular momentum converges to the same integral value. This demonstrates that the ground state derived in Sec. II can indeed be prepared by the time-dependent stirring potential in the presence of energy dissipation, and that the circulation is indeed quantized in the thermodynamically stable state.

From these results, it is concluded that the system reaches a thermodynamically stable state after both density fluctuations and energy dissipation. The density oscillation is dras-

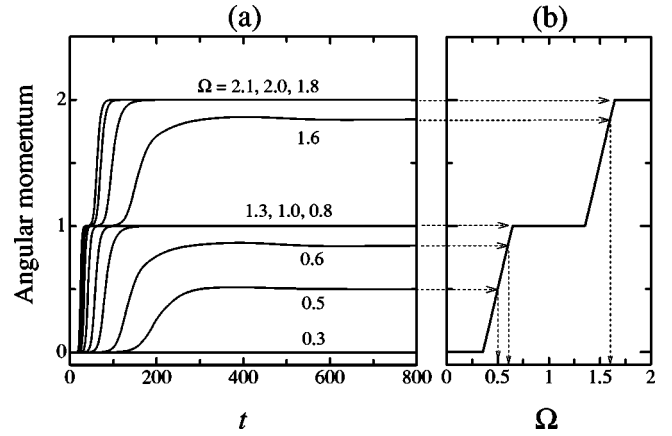


FIG. 10. (a) Time evolution of the angular momentum of an initially uniform state with a damping constant  $\Gamma = 0.1$  for  $\gamma = -1/4$  and  $V_0 = 10^{-3}$ . (b) Expectation value of angular momentum per atom obtained by the MFT for  $\gamma = -1/4$ .

tically enhanced near the resonant frequency. However, energy must be dissipated in order for the system to acquire a net and thermodynamically stable angular momentum. Similar mechanisms have been found in the vortex lattice formation [13].

## VI. CONCLUSIONS

We investigated the rotational properties of one-dimensional bosons with attractive interactions confined in a rotating torus trap.

We derived the ground-state wave function analytically within the MFT as a function of the strength of interaction  $\gamma$  and of the rotational frequency of the torus  $\Omega$ . A uniform-density solution and a bright-soliton one were found to cross over each other smoothly. The density of the soliton depends on the rotational frequency  $\omega$  and has a node at  $\Omega = J + 1/2$  when a vortex enters the ring.

In order to investigate the validity of the Bogoliubov theory, we compared the excitation spectrum obtained by the Bogoliubov theory with that obtained by the exact diagonalization of the many-body Hamiltonian. We found that the MFT well describes the ground state and the low-lying excited states, except for  $\Omega \approx J, \gamma = -1/2$ , where the phase boundary coincides with the borderline of the onset of dynamical instability, thereby producing significant quantum fluctuations.

The angular momentum of the ground state is quantized with respect to  $\Omega$  in the uniform-density regime, but it is not quantized in the soliton regime. The circulations at finite temperature were examined by the exact diagonalization method, and an experimental situation to realize our predictions was discussed.

To understand the process by which the system is set into rotation, we considered a time-dependent stirring potential that breaks the axisymmetry of the torus. The potential was shown to induce the resonance, causing the density to oscillate and thus triggering the system to acquire angular momentum. However, energy must be dissipated in order for the

circulation to acquire a thermodynamically stabilized quantized value.

### ACKNOWLEDGMENTS

This research was supported by a Grant-in-Aid for Scientific Research (Grant No. 15340129), by Special Coordination Funds for Promoting Science and Technology from the Ministry of Education, Culture, Sports, Science and Technology of Japan, and by the Yamada Science Foundation.

### APPENDIX A: ELLIPTIC INTEGRALS AND ELLIPTIC FUNCTIONS

Definitions and inter-relations of some elliptic integrals and elliptic functions [27] appearing in this paper are summarized as follows.

Elliptic integrals of the first kind  $F$ , the second kind  $E$ , and the third kind  $\Pi$  are defined as

$$F(\phi/\alpha) \equiv \int_0^\phi \frac{d\theta}{\sqrt{1 - \sin^2 \alpha \sin^2 \theta}}, \quad (\text{A1})$$

$$E(\phi/\alpha) \equiv \int_0^\phi d\theta \sqrt{1 - \sin^2 \alpha \sin^2 \theta}, \quad (\text{A2})$$

$$\Pi(n; \phi/\alpha) \equiv \int_0^\phi \frac{d\theta}{(1 - n \sin^2 \theta) \sqrt{1 - \sin^2 \alpha \sin^2 \theta}}. \quad (\text{A3})$$

Using a parameter  $m \equiv \sin^2 \alpha$ , Jacobian elliptic functions are defined by

$$\text{sn}(u|m) \equiv \sin \phi, \quad (\text{A4})$$

$$\text{cn}(u|m) \equiv \cos \phi, \quad (\text{A5})$$

$$\text{dn}(u|m) \equiv \sqrt{1 - m \sin^2 \phi}, \quad (\text{A6})$$

and these functions are inter-related as

$$\text{dn}^2(u|m) - m_1 = m \text{cn}^2(u|m) = m[1 - \text{sn}^2(u|m)]. \quad (\text{A7})$$

Using the parameter set  $\{u, m\}$  instead of  $\{\phi, \alpha\}$ , the elliptic integrals are also expressed as

$$F(u|m) \equiv \int_0^u dv = u, \quad (\text{A8})$$

$$E(u|m) \equiv \int_0^u \text{dn}^2(v|m) dv, \quad (\text{A9})$$

$$\Pi(n; u|m) \equiv \int_0^u \frac{dv}{1 - n \text{sn}^2(v|m)}. \quad (\text{A10})$$

Elliptic integrals are said to be complete when  $\phi = \pi/2$ , and are usually denoted as

$$K(m) \equiv F\left(\frac{\pi}{2} \middle| m\right), \quad E(m) \equiv E\left(\frac{\pi}{2} \middle| m\right). \quad (\text{A11})$$

Complete elliptic integrals of the first and second kinds are expanded for  $|m| < 1$  as infinite series

$$K(m) = \frac{\pi}{2} \left[ 1 + \left(\frac{1}{2}\right)^2 m + \left(\frac{1 \cdot 3}{2 \cdot 4}\right)^2 m^2 + \left(\frac{1 \cdot 3 \cdot 5}{2 \cdot 4 \cdot 6}\right)^2 m^3 + \dots \right], \quad (\text{A12})$$

$$E(m) = \frac{\pi}{2} \left[ 1 - \left(\frac{1}{2}\right)^2 m - \left(\frac{1 \cdot 3}{2 \cdot 4}\right)^2 \frac{m^2}{3} - \left(\frac{1 \cdot 3 \cdot 5}{2 \cdot 4 \cdot 6}\right)^2 \frac{m^3}{5} - \dots \right]. \quad (\text{A13})$$

The elliptic integral of the third kind  $\Pi(n; \phi/\alpha)$  has other expressions depending on the relation between  $m$  and  $n$ . When  $m < n < 1$  and  $\phi = \pi/2$ , it reduces to

$$\Pi\left(n; \frac{\pi}{2} \middle| \alpha\right) = K(\alpha) + \frac{\pi}{2} \delta_2 \{1 - \Lambda_0(\varepsilon/\alpha)\}, \quad (\text{A14})$$

$$\delta_2 \equiv \sqrt{\frac{n}{(1-n)(n - \sin^2 \alpha)}}, \quad (\text{A15})$$

$$\varepsilon \equiv \arcsin \sqrt{\frac{1-n}{\cos^2 \alpha}}, \quad (\text{A16})$$

where  $\Lambda_0$  is Heuman's lambda function defined as

$$\Lambda_0(\phi/\alpha) \equiv \frac{2}{\pi} [K(\alpha)E(\phi/90^\circ - \alpha) - \{K(\alpha) - E(\alpha)\}F(\phi/90^\circ - \alpha)]. \quad (\text{A17})$$

### APPENDIX B: LIMITING BEHAVIORS OF THE SOLITON SOLUTIONS

We consider the limits  $|\omega| \rightarrow 0$  and  $|\omega| \rightarrow 1/2$  of the soliton solution for  $0 < |\omega| < 1/2$  given by

$$\rho(\theta) = \frac{K^2}{\pi^3 |\gamma|} \left[ \text{dn}^2 \left( \frac{K}{\pi} (\theta - \theta_0) \middle| m \right) - \eta m_1 \right], \quad (\text{B1})$$

$$\varphi(\theta) = \Omega \theta - \text{sgn}(\omega) \delta_2^{-1} \Pi \left( n; \frac{K\theta}{\pi} \middle| m \right), \quad (\text{B2})$$

$$\mu = \frac{1}{2\pi^2} (f_d - f_c - f), \quad (\text{B3})$$

where

$$f \equiv 2K^2 - 2KE - \pi^2 \gamma, \quad (\text{B4})$$

$$f_c \equiv 2m_1 K^2 - 2KE - \pi^2 \gamma, \quad (\text{B5})$$

$$f_d \equiv 2KE + \pi^2 \gamma. \quad (\text{B6})$$

The limiting values and behaviors of several parameters are summarized in Table I and Fig. 11, respectively. In the limit  $|\omega| \rightarrow 0$  ( $f_d \rightarrow 0$ ), Eqs. (B1) and (B2) continuously become the dn solution, since  $\eta \rightarrow 0$  and  $W \rightarrow 0$ , as seen from

TABLE I. Limiting values of various parameters of the soliton solution. The limit  $|\omega| \rightarrow 0$  is equivalent to the limit  $f_{dn} \rightarrow 0$  or  $\gamma \rightarrow -2KE/\pi^2 - 0$ , and  $|\omega| \rightarrow 0.5$  is equivalent to  $f_{cn} \rightarrow 0$  or  $\gamma \rightarrow -2(KE - m_1 K^2)/\pi^2 - 0$ . The limit  $m \rightarrow 0$  corresponds to the uniform-density limit of  $|\gamma| \rightarrow -2\omega^2 + 1/2 + 0$ .

	$ \omega  \rightarrow 0$	$ \omega  \rightarrow 0.5$	$m \rightarrow 0$
$\eta$	0	1	$1 + 2\gamma$
$n$	$m$	1	0
$W^2$	0	0	$\sqrt{1 + 2\gamma}/4\pi$
$\delta_2$	$\infty$	$\infty$	$\sqrt{1/(1 + 2\gamma)}$
$\varepsilon$	$\pi/2$	0	$\pi/2$

Fig. 11 and Table I. In the limit  $|\omega| \rightarrow 1/2$  ( $f_c \rightarrow 0$ ), where the parameters behave as  $\eta \rightarrow 1$ ,  $W \rightarrow 0$ , Eqs. (B1) and (B2) reproduce the cn solution. It can easily be verified by setting  $f_d = 0$  or  $f_c = 0$  in Eq. (B3) that in these limits the chemical potential for  $0 < |\omega| < 1/2$  continuously approaches

$$\mu = -\frac{K^2}{\pi^2}(1 + m_1) = \frac{1}{2\pi^2}(-f_c - f), \quad |\omega| = 0, \quad (\text{B7})$$

$$\mu = -\frac{K^2}{\pi^2}(1 - 2m_1) = \frac{1}{2\pi^2}(f_d - f), \quad |\omega| = 1/2. \quad (\text{B8})$$

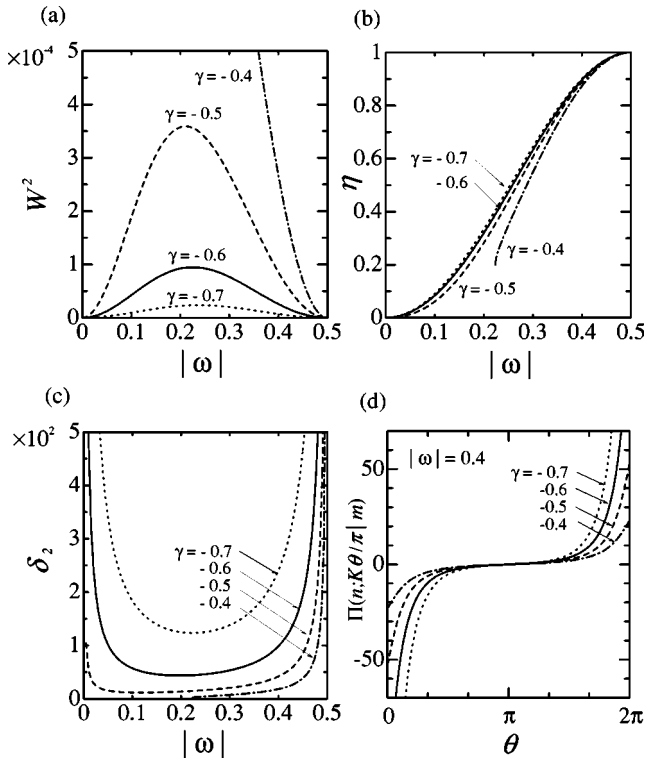


FIG. 11. (a)–(c) Behaviors of several parameters appeared in the soliton solution for  $\gamma = -0.4$  (dashed-and-dotted),  $\gamma = -0.5$  (dashed),  $\gamma = -0.6$  (solid), and  $\gamma = -0.7$  (dotted curves). (d) Incomplete elliptic integral of the third kind  $\Pi(n; K\theta/\pi|m)$  for  $|\omega| = 0.4$  as a function of  $\theta$ .

The first derivative of the ground-state energy with respect to  $\Omega$  has a kink at the phase boundary, which is verified by relations (58) and (59) as

$$\frac{\partial \mathcal{E}}{\partial \Omega} = 2(\Omega - \langle \hat{L} \rangle_0 / N) = \begin{cases} 0, & |\omega| = 0, 1/2, \\ -4\pi W, & 0 < |\omega| < 1/2. \end{cases} \quad (\text{B9})$$

Figure 12 shows the solution  $m$  calculated numerically by solving

$$f_d = 0, \quad |\omega| = 0, \\ 2\pi|\omega| = \sqrt{\frac{2f_d f_c}{f}} + \pi(1 - \Lambda_0), \quad 0 < |\omega| < 1/2, \quad (\text{B10})$$

$$f_c = 0, \quad |\omega| = 1/2,$$

where the line of intersection between the curves and the  $\gamma$ - $\omega$  plane corresponds to the phase boundary  $\gamma - 2\omega^2 + 1/2 = 0$ .

### APPENDIX C: GROUND-STATE PROPERTIES NEAR THE PHASE BOUNDARY

We investigate the continuity of the ground-state properties at the phase boundary. From Fig. 12, we see that the parameter  $m$  becomes zero for all soliton solutions in the limit  $|\gamma| \rightarrow -2\omega^2 + 1/2 + 0$ . The uniform-density limit of the soliton solution is hence mathematically obtained by taking the limit of  $m \rightarrow 0$ . Let  $\delta$  be a positive small deviation of  $\gamma$  from the value at the phase boundary for a fixed  $\omega$ . For  $|\omega| = 0, 1/2$ , the parameter  $m$ , the complete elliptic integrals  $K(m), E(m)$ , and hence the physical quantities near the phase boundary are expanded in terms of  $\delta$  in the following manner.

For the dn solution ( $\omega = 0$ ), the phase boundary is  $\gamma = -1/2$  and let  $\gamma = -1/2 - \delta$ . Using the equation  $f_d = 0$ , we obtain

$$m = 8\delta^{1/2} - 32\delta + 89\delta^{3/2} - 200\delta^2 + O(\delta^{5/2}). \quad (\text{C1})$$

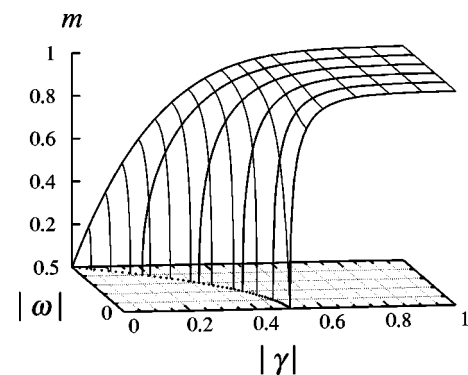


FIG. 12. The solution  $m$  calculated numerically from Eq. (B10). The dotted curve on the  $\omega$ - $\gamma$  plane represents the phase boundary  $\gamma - 2\omega^2 + 1/2 = 0$ , and there exists a unique solution  $m$  in the soliton regime  $|\gamma| > -2\omega^2 + 1/2$ .

The expansion formulas (A12) and (A13) become

$$K = \frac{\pi}{2} \left( 1 + 2\delta^{1/2} + \delta + \frac{1}{4}\delta^{3/2} + \frac{1}{2}\delta^2 \right) + O(\delta^{5/2}), \quad (\text{C2})$$

$$E = \frac{\pi}{2} \left( 1 - 2\delta^{1/2} + 5\delta - \frac{33}{4}\delta^{3/2} + \frac{23}{2}\delta^2 \right) + O(\delta^{5/2}). \quad (\text{C3})$$

Using these expansions, the ground-state energy and the chemical potential are expressed as functions of  $\delta$  instead of  $m$  near the phase boundary  $\gamma = -1/2 - \delta$ . The jump in the second derivative of the ground-state energy and that in the first derivative of the chemical potential are obtained as

$$\mathcal{E}'_{\text{dn}} - \mathcal{E}'_{\text{u}} = -4, \quad \mu'_{\text{dn}} - \mu'_{\text{u}} = -2, \quad (\text{C4})$$

at  $\gamma = -1/2$  and  $\omega = 0$ .

For the cn solution ( $|\omega| = 1/2$ ) at  $\gamma = -\delta$ , the expansions are obtained in a similar way, as

$$m = 4\delta - 6\delta^2 + O(\delta^3), \quad (\text{C5})$$

$$K = \frac{\pi}{2} \left( 1 + \delta + \frac{3}{4}\delta^2 \right) + O(\delta^3), \quad (\text{C6})$$

$$E = \frac{\pi}{2} \left( 1 - \delta + \frac{3}{4}\delta^2 \right) + O(\delta^3). \quad (\text{C7})$$

The ground-state energy and the chemical potential are expanded in terms of  $\delta$  as

$$\mathcal{E}_{\text{cn}} = \frac{1}{4} - \frac{3\delta}{4} - \frac{\delta^2}{8} + O(\delta^3), \quad (\text{C8})$$

$$\mu_{\text{cn}} = \frac{1}{4} - \frac{3\delta}{2} - \frac{3\delta^2}{8} + O(\delta^3), \quad (\text{C9})$$

which are continuously connected with those of the uniform-density solution at  $\gamma = 0$  and  $|\omega| = 1/2$ . However, the first derivative of the ground-state energy and that of the chemical potential are given by

$$\mathcal{E}'_{\text{cn}} = -\frac{3}{4} - \frac{\delta}{4} + O(\delta^2), \quad (\text{C10})$$

$$\mu'_{\text{cn}} = -\frac{3}{2} - \frac{3\delta}{4} + O(\delta^2), \quad (\text{C11})$$

and have discontinuous jumps at  $\gamma = 0$  and  $|\omega| = 1/2$  by the following amounts:

$$\mathcal{E}'_{\text{cn}} - \mathcal{E}'_{\text{u}} = -\frac{1}{4}, \quad \mu'_{\text{cn}} - \mu'_{\text{u}} = -\frac{1}{2}. \quad (\text{C12})$$

- 
- [1] C. Raman, J.R. Abo-Shaeer, J.M. Vogels, K. Xu, and W. Ketterle, *Phys. Rev. Lett.* **87**, 210402 (2001).
- [2] A. Görlitz, J.M. Vogels, A.E. Leanhardt, C. Raman, T.L. Gustavson, J.R. Abo-Shaeer, A.P. Chikkatur, S. Gupta, S. Inouye, T. Rosenband, and W. Ketterle, *Phys. Rev. Lett.* **87**, 130402 (2001).
- [3] F. Schreck, L. Khaykovich, K.L. Corwin, G. Ferrari, T. Bourdel, J. Cubizolles, and C. Salomon, *Phys. Rev. Lett.* **87**, 080403 (2001).
- [4] M. Greiner, I. Bloch, O. Mandel, T.W. Hänsch, and T. Esslinger, *Phys. Rev. Lett.* **87**, 160405 (2001).
- [5] L. Khaykovich, F. Schreck, G. Ferrari, T. Bourdel, J. Cubizolles, L.D. Carr, Y. Castin, and C. Salomon, *Science* **296**, 1290 (2002).
- [6] K.E. Strecker, G.B. Partridge, A.G. Truscott, and R.G. Hulet, *Nature (London)* **417**, 150 (2002).
- [7] F. Bloch, *Phys. Rev. A* **7**, 2187 (1973).
- [8] V.A. Kashurnikov, A.I. Podlivaev, N.V. Prokof'ev, and B.V. Svistunov, *Phys. Rev. B* **53**, 13 091 (1996).
- [9] D.S. Rokhsar, e-print cond-mat/9709212.
- [10] M. Ueda and A.J. Leggett, *Phys. Rev. Lett.* **83**, 1489 (1999).
- [11] Y. Kagan, N.V. Prokof'ev, and B.V. Svistunov, *Phys. Rev. A* **61**, 045601 (2000).
- [12] K. Kasamatsu, M. Tsubota, and M. Ueda, *Phys. Rev. A* **66**, 053606 (2002).
- [13] K. Kasamatsu, M. Tsubota, and M. Ueda, *Phys. Rev. A* **67**, 033610 (2003).
- [14] V.E. Zakharov and A.B. Shabat, *Zh. Éksp. Teor. Fiz.* **61**, 118 (1971) [*Sov. Phys. JETP* **34**, 62 (1972)].
- [15] L.D. Carr, C.W. Clark, and W.P. Reinhardt, *Phys. Rev. A* **62**, 063611 (2000).
- [16] H. Saito and M. Ueda, *Phys. Rev. Lett.* **90**, 040403 (2003).
- [17] F.Kh. Abdullaev, J.G. Caputo, R.A. Kraenkel, and B.A. Malomed, *Phys. Rev. A* **67**, 013605 (2003).
- [18] T. Kuga, Y. Torii, N. Shiokawa, T. Hirano, Y. Shimizu, and H. Sasada, *Phys. Rev. Lett.* **78**, 4713 (1997).
- [19] E.H. Lieb and W. Liniger, *Phys. Rev.* **130**, 1605 (1963); E.H. Lieb, *ibid.* **130**, 1616 (1963).
- [20] G.B. Hess and W.M. Fairbank, *Phys. Rev. Lett.* **19**, 216 (1967).
- [21] L. Onsager, *Nuovo Cimento, Suppl.* **6**, 249 (1949).
- [22] R.P. Feynman, *Prog. Low Temp. Phys.* **1**, 17 (1995).
- [23] R. Kanamoto, H. Saito, and M. Ueda, *Phys. Rev. A* **67**, 013608 (2003).
- [24] G.M. Kavoulakis, *Phys. Rev. A* **67**, 011601(R) (2003).
- [25] A.J. Leggett, *Low Temperature Physics*, edited by M.J.R. Hoch and R.H. Lemmer (Springer-Verlag, Berlin, 1991).
- [26] A.J. Leggett, *Phys. Fenn.* **8**, 125 (1973).
- [27] *Handbook of Mathematical Functions*, edited by M. Abramowitz and I.A. Stegun (Dover, New York, 1965).
- [28] P.F. Kartsev, e-print cond-mat/0211356.
- [29] E.J. Mueller, *Phys. Rev. A* **66**, 063603 (2002).
- [30] W. Hänsel, P. Hommelhoff, T.W. Hänsch, and J. Reichel, *Nature (London)* **413**, 498 (2001).
- [31] S. Choi, S.A. Morgan, and K. Burnett, *Phys. Rev. A* **57**, 4057 (1998).
- [32] M. Tsubota, K. Kasamatsu, and M. Ueda, *Phys. Rev. A* **65**, 023603 (2002).